

IMAGING ASSESSMENT AND FEASIBILITY OF A HYDROSTATICALLY ACTUATED ROBOTIC SYSTEM FOR REAL-TIME MRI-GUIDED INTERVENTIONS

Samantha Mikael^{1,2}, Rashid Yasin³, Samuel Ross⁴, M. Wasi Wahi-Anwar¹, James Simonelli³, David Lu², Kyung Sung^{1,2}, Tsu-Chin Tsao³, and Holden H. Wu^{1,2}

¹Biomedical Physics, University of California Los Angeles, Los Angeles, CA, United States, ²Radiological Sciences, University of California Los Angeles, Los Angeles, CA, United States, ³Mechanical and Aerospace Engineering, University of California, Los Angeles, CA, United States, ⁴Santa Monica College, Santa Monica, CA, United States

Introduction: Real-time image visualization and guidance are crucial to the success of minimally invasive cancer interventions, especially in the abdomen. MRI provides exceptional soft tissue contrast without ionizing radiation and can visualize lesions that are poorly depicted or invisible on ultrasound and/or computed tomography^[1]. Therefore, MRI is an ideal technology for real-time image guidance during interventions. However, MRI-guided interventions have limited access to the patient inside closed-bore MRI scanners. A common work-around is to move the patient in and out of the scanner for intermittent imaging and intervention, which compromises the real-time capability of MRI for guiding interventions and prolongs procedure time. In this work, we present a new robotic system prototype based on hydrostatic actuation that enables 3-degree-of-freedom (DOF) remote control of interventional devices inside the scanner bore under real-time MRI guidance (Fig. 1). We evaluate its effects on MR image artifact, signal-to-noise ratio (SNR), and distortion. Furthermore, we investigate the feasibility of our new robotic system for 3-DOF control and targeted needle placement under real-time MRI guidance.

Methods: [System Design] The MRI-compatible master-slave robotic system was developed using low-pressure water-based hydrostatic actuators^[2]. The system uses piston pairs connected to closed fluid channels, which transmits force and displacement into the bore of the scanner. The channels are five to six feet in length, which can provide haptic feedback with minimal loss and allows devices to be inside the bore while the physician manipulates the system from the end of the patient table. Polypropylene was used for construction to reduce cost and avoid adverse imaging effects. [Imaging Assessment] All experiments were performed on a 3 T MRI scanner (TIM Trio, Siemens). The robotic system was equipped with an MRI-compatible biopsy needle (Cook), and placed in the bore next to a sphere phantom. Gradient echo (GRE), fast spin echo (FSE), and balanced steady state free precession (bSSFP) scans of the phantom were obtained. The scans were then repeated without the robotic system. Images were inspected for artifacts. The SNR was calculated using the two-scan difference method^[3]. The entire process was repeated with a grid phantom, where dimensions of the imaged grid lines with and without the robotic system were measured to assess distortion. [Feasibility] Based on visualization from a real-time GRE sequence at 2 frames/second, an operator controlled the robotic system from the end of the patient table to evaluate MRI-guided 3-DOF manipulation of the needle in a gelatin phantom. Following the same setup, feasibility of targeted needle placement was evaluated in a gelatin phantom with embedded contrast beads. Before targeting, the phantom was imaged with a 3D GRE sequence and the target positions were defined. The operator then remotely controlled the robotic system and adjusted the trajectory of the needle in real-time based on MRI visual guidance to approach and finally arrive at the target. After the operator was satisfied with needle placement, the phantom was imaged again with a 3D GRE sequence for validation. This was repeated for each defined target.

Results: [Imaging Assessment] No image artifacts were observed with the robotic system inside the scanner (images not shown). The SNR difference between the phantom with the robotic system to the phantom is on average only -2.2% for all three sequences. The grid phantom images showed no distortion. [Feasibility] The operator was able to easily position and insert a biopsy needle in the phantom from the end of the patient table repeatedly, in all three DOF (Fig. 2). Figure 2b demonstrates insertion in the sagittal plane, while Figure 2c demonstrates translation across y followed by x in the coronal plane. For the needle targeting experiments, the operator was successful in reaching all three defined targets, which were evenly separated by 5.5 mm along the surface of the contrast bead (Fig. 3). The average difference between the final position of the needle tip and defined targets was 1.34 mm (range of 1.08-1.56 mm).

Discussion and Conclusion: Our proposed MRI-compatible robotic system exhibits negligible impact on image artifact, SNR, and distortion. Furthermore, it can successfully transmit force and displacement in all three DOF into the closed bore under real-time MRI guidance. Using our new robotic system, the operator was able to remotely guide the needle to all of the targets with relative ease. Clinically, physicians target lesions as small as 5 mm with a desired accuracy of <2 mm, and initial results demonstrate feasibility for our robotic system to attain this accuracy. In addition to MRI visual guidance, the operator could rely on haptic feedback from our system to confirm needle placement at the target. Our new MRI-compatible robotic system can potentially provide physicians continuous access to patients during real-time MRI-guided interventions with improved visualization and accuracy.

References: ^[1]Rothgang et al., JMIR 2013, 37:1202-12; ^[2]Yasin et al., Proc 10th iMRI Symposium 2014, p.41; ^[3]Dietrich et al., JMIR 2007, 26:375-85

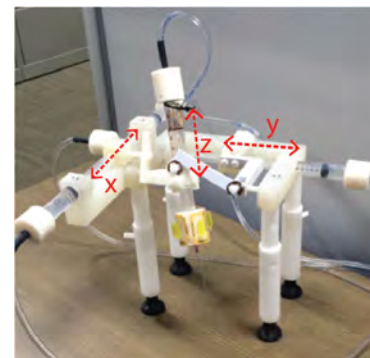


Fig 1: Robotic system prototype that fully enables 3-DOF control (arrows)

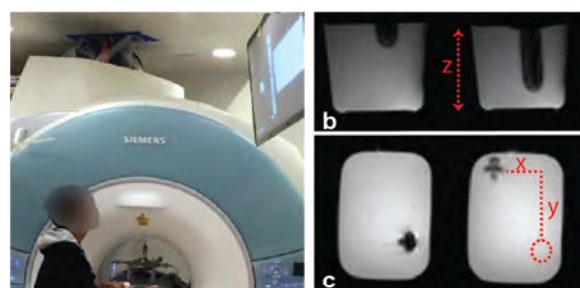


Fig 2: (a) Operator manipulates robotic system from end of patient bed. Real-time MRI of (b) insertion along z and (c) translation along xy.

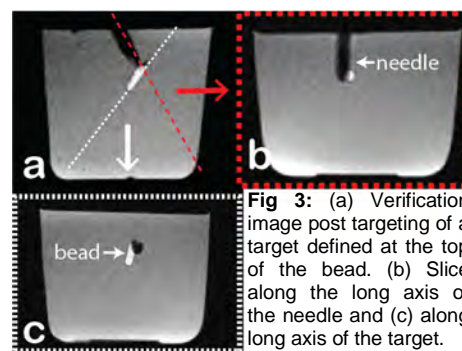


Fig 3: (a) Verification image post targeting of a target defined at the top of the bead. (b) Slice along the long axis of the needle and (c) along long axis of the target.